

A New Inorganic–Organic Photoluminescent Material Constructed with Helical $[\text{Zn}_3(\mu_3\text{-OH})(\mu_2\text{-OH})]$ Chains

Jun Tao, Jian-Xin Shi, Ming-Liang Tong,*
Xiao-Xia Zhang, and Xiao-Ming Chen*

State Key Laboratory of Ultrafast Laser Spectroscopy,
School of Chemistry & Chemical Engineering, Zhongshan
University, Guangzhou, 510275, P.R. China

Received May 3, 2001

Introduction

Coordination polymers formed through the deliberate selection of metals and multifunctional exodentate ligands, based upon their coordination habits, have so far spawned tremendous interest in the area of materials chemistry. The fascinating structures of these complexes, coupled with their specific functionality, have made them highly promising in various applications, particularly absorption, catalysis, and molecular magnetization.^{1,2} While an enormous amount of current research is being focused on the synthesis and structure characterization of mononuclear or dinuclear transition metal coordination polymers, less attention has been paid to the construction of coordination polymers with transition metal polynuclear clusters.³ Polynuclear clusters exhibit a variety of coordination motifs that can be exploited in materials science owing to their rigidity and intriguing physical properties. Polynuclear clusters can be synthesized by the hydrolysis or alcoholysis of metal salts in the presence of templating ligands.⁴ These compounds feature hydrophilic groups within the core, a necessary requirement for the core to aggregate. Our recent studies on the synthesis of zinc-based complexes under hydrothermal conditions have shown that the use of Zn_4O and $\text{Zn}_4(\text{OH})_2$ clusters as the rigid secondary building units leads to multidimensional

frameworks.⁵ We report herein the preparation, crystal structure, and luminescent properties of a 3-D coordination polymer with helical chains of OH-bridged basic trizinc clusters, namely, $[\text{Zn}_3(\mu_3\text{-OH})(\mu_2\text{-OH})(4,4'\text{-bpy})_{0.5}(4,4'\text{-oba})_2] \cdot 0.5\text{H}_2\text{O}$ (4,4'-bpy = 4,4'-bipyridine; 4,4'-oba = 4,4'-oxybis(benzoate)) (1).

Experimental Section

All reagents were commercially available and used as received. The C, H, N microanalyses were carried out with a Perkin-Elmer 240 elemental analyzer. The FT-IR spectra were recorded from KBr pellets in the range 4000–400 cm^{-1} on a Nicolet 5DX spectrometer. For low-temperature photoluminescence measurement, samples were mounted in a closed-cycle cryostat in which the temperature can be adjusted from 10 to 300 K. The 325 nm line of a He–Cd laser was used as an excitation source. The emission light was collected and dispersed by a 0.25 m double monochromator with a water-cooled photomultiplier tube and processed with a lock-in amplifier. The room-temperature emission and excitation spectra were carried out using a Hitachi F-4500 spectrofluorometer. The excitation spectra were measured over the 235–400 nm wavelength range, the emission intensity being monitored at 415 and 465 nm, respectively. The emission spectra were measured using variable excitation wavelengths.

Synthesis of $[\text{Zn}_3(\mu_3\text{-OH})(\mu_2\text{-OH})(4,4'\text{-bpy})_{0.5}(4,4'\text{-oba})_2] \cdot 0.5\text{H}_2\text{O}$ (1). An aqueous mixture (8 cm^3) containing $\text{Zn}(\text{NO}_3)_2 \cdot 6\text{H}_2\text{O}$ (0.158 g, 0.50 mmol), 4,4'-bpy (0.078 g, 0.50 mmol), 4,4'-oba (0.128 g, 0.50 mmol), and NaOH (0.06 g, 1.5 mmol) was placed in a Parr Teflon-lined stainless steel vessel (23 cm^3), and the vessel was sealed, heated to 180 °C for 7 days, and then cooled at 5 °C/h to 100 °C and held for 10 h, followed by slow cooling to room temperature. Colorless block crystals were collected in ca. 60% yield based on $\text{Zn}(\text{NO}_3)_2$. Calcd for $\text{C}_{33}\text{H}_{23}\text{NO}_{12.5}\text{Zn}_3$: C, 47.77, H, 2.79, N, 1.69%. Found: C, 48.91, H, 2.70, N 1.71. IR data (cm^{-1}): 3391 (m), 1598 (s), 1559 (s), 1499 (m), 1409 (s), 1386 (s), 1300 (w), 1247 (s), 1159 (m), 1097 (w), 1071 (w), 1011 (w), 876 (m), 782 (m), 641 (w).

X-ray Crystallography. Diffraction intensities for the complex were collected at 21 °C on a Siemens R3m diffractometer using the ω -scan technique. Lorentz-polarization and absorption corrections were applied.⁶ The structure was solved with direct methods and refined with full-matrix least-squares techniques using the SHELXS-97 and SHELXL-97 programs, respectively.^{7,8} Non-hydrogen atoms were refined anisotropically. The organic hydrogen atoms were generated geometrically (C–H = 0.96 Å); the aqua hydrogen atoms were located from difference maps and refined with isotropic temperature factors. Analytical expressions of neutral-atom scattering factors were employed, and anomalous dispersion corrections were incorporated.⁹ The crystallographic data for **1** is listed in Table 1; selected bond lengths (Å) and bond angles (deg) are given in Table 2. Drawings were produced with SHELXTL.¹⁰

Results and Discussion

Crystal Structure. A single-crystal X-ray diffraction study of **1** reveals an infinite 3D coordination polymer that crystallizes in the space group $C2/c$. The basic building block of **1** is a “basic” trizinc carboxylate with three crystallographically

* Correspondence should be addressed directly to the School of Chemistry. E-mail: cestml@zsu.edu.cn (M.-L.T.) and cesxcm@zsu.edu.cn (X.-M.C.).

- (1) (a) Sato, O.; Iyoda, T.; Fujishima, A.; Hashimoto, K. *Science* **1996**, *271*, 49. (b) Chui, S. S.-Y.; Lo, S. M.-F.; Charmant, J. P. H.; Orpen, A. G.; Williams, I. D. *Science* **1999**, *283*, 1148. (c) Evans, O. R.; Xiong, R.; Wang, R.; Wong, G. K.; Lin, W. *Angew. Chem., Int. Ed.* **1999**, *38*, 536. (d) Carlucci, L.; Ciani, G.; Proserpio, D. M.; Sironi, A. *J. Chem. Soc., Chem. Commun.* **1994**, 2755. (e) Yaghi, O. M.; Li, H.; Davis, C.; Richardson, D.; Groy, T. L. *Acc. Chem. Res.* **1998**, *31*, 575. (f) Hargman, P. J.; Hargman, D.; Zubieta, J. *Angew. Chem., Int. Ed.* **1999**, *38*, 2638, and references therein. (g) Eddaoudi, M.; Li, H.; Yaghi, O. M. *J. Am. Chem. Soc.* **2000**, *122*, 1391. (h) Noro, S.; Kitagawa, S.; Kondo, M.; Seki, K. *Angew. Chem., Int. Ed.* **2000**, *39*, 2081.
- (2) (a) Tong, M.-L.; Chen, X.-M.; Ye, B.-H.; Ji, L.-N. *Angew. Chem., Int. Ed.* **1999**, *38*, 2237. (b) Tong, M.-L.; Zheng, S.-L.; Chen, X.-M. *Chem. Commun.* **1999**, 561. (c) Tong, M.-L.; Chen, H.-J.; Chen, X.-M. *Inorg. Chem.* **2000**, *39*, 2235. (d) Tong, M.-L.; Zheng, S.-L.; Chen, X.-M. *Chem. Eur. J.* **2000**, *6*, 3729. (e) Zheng, S.-L.; Tong, M.-L.; Fu, R.-W.; Chen, X.-M.; Ng, S. W. *Inorg. Chem.* **2001**, *40*, 3562 and references therein.
- (3) (a) Li, H.; Eddaoudi, M.; O’Keeffe, M.; Yaghi, O. M. *Nature* **1999**, *402*, 276. (b) Ma, B.-Q.; Zhang, D.-S.; Gao, S.; Jin, T.-Z.; Yan, C.-H.; Xu, G.-X. *Angew. Chem., Int. Ed.* **2000**, *39*, 3644.
- (4) (a) Blake, A. J.; Grant, C. M.; Parsons, S.; Rawson, J. M.; Winpenny, R. E. P. *J. Chem. Soc., Chem. Commun.* **1994**, 2363. (b) Watton, S. P.; Fuhrmann, P.; Pence, L. E.; Caneschi, A.; Cormia, A.; Abbati, G. L.; Lippard, S. J. *Angew. Chem., Int. Ed. Engl.* **1997**, *36*, 2774.

- (5) Tao, J.; Tong, M.-L.; Shi, J.-X.; Chen, X.-M.; Ng, S. W. *Chem. Commun.* **2000**, 2043.
- (6) North, A. C. T.; Phillips, D. C.; Mathews, F. S. *Acta Crystallogr., Sect. A* **1968**, *24*, 351.
- (7) Sheldrick, G. M. *SHELXS-97, Program for Crystal Structure Solution*; University of Göttingen: Göttingen, Germany, 1997.
- (8) Sheldrick, G. M. *SHELXL-97, Program for Crystal Structure Refinement*; University of Göttingen: Göttingen, Germany, 1997.
- (9) *International Tables for X-ray Crystallography*; Kluwer Academic Publisher: Dordrecht, 1992; Vol. C, Tables 4.2.6.8 and 6.1.1.4.
- (10) Sheldrick, G. M. *SHELXTL*, version 5; Siemens Industrial Automation Inc.: Madison, WI, 1995.

Table 1. Crystallographic and Experimental Data for **1**

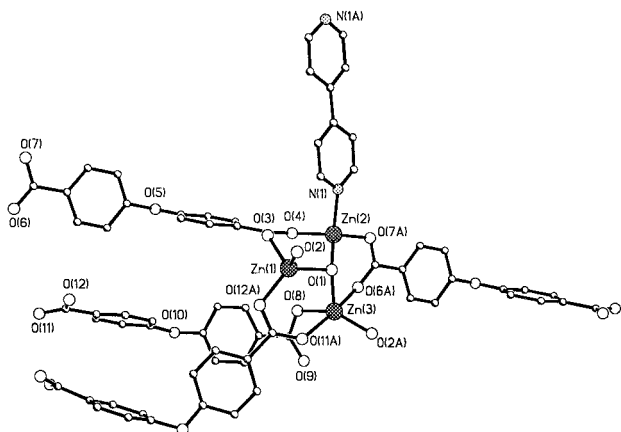
formula	$C_{33}H_{23}NO_{12.50}Zn_3$	<i>Z</i>	8
fw	829.63	ρ_{calcd} (g cm ⁻³)	1.677
cryst syst	monoclinic	<i>T</i> (°C)	21
space group	<i>C2/c</i>	λ (Mo K α) (Å)	0.71073
<i>a</i> (Å)	28.419(14)	μ (Mo K α) (mm ⁻¹)	2.240
<i>b</i> (Å)	9.572(3)	R1 (<i>I</i> > 2 σ (<i>I</i>)) ^a	0.0464
<i>c</i> (Å)	24.162(13)	wR2 (all data) ^a	0.0999
β (deg)	90.78(2)		

$$^a R1 = \frac{\sum ||F_o| - |F_c||}{\sum |F_o|}, wR2 = \frac{[\sum w(F_o^2 - F_c^2)^2 / \sum w(F_o^2)]^{1/2}}{w} = \frac{[\sigma^2(F_o^2) + (0.1(\max(0, F_o^2) + 2F_c^2/3))^2]^{-1/2}}$$

Table 2. Selected Bond Distances (Å) and Angles (deg) for **1**

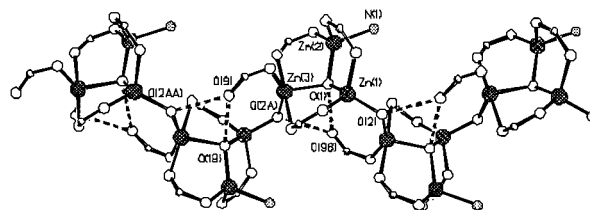
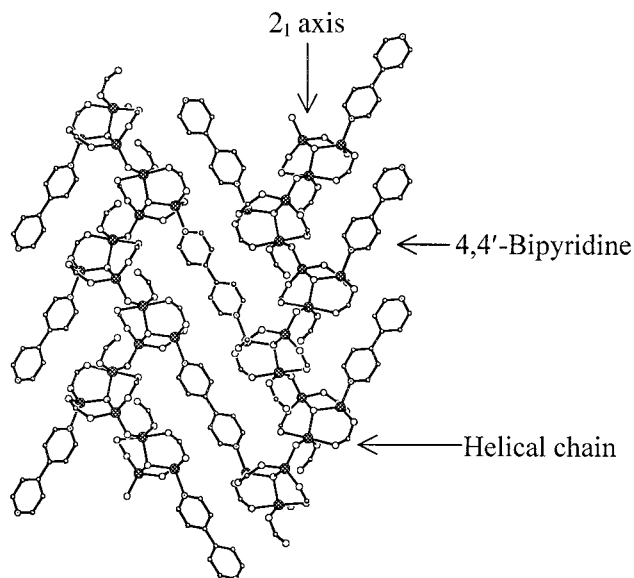
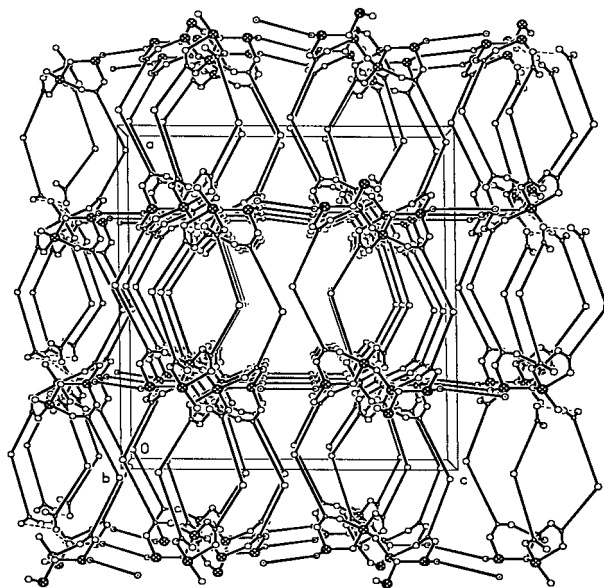
Zn(1)–O(1)	2.019(3)	Zn(2)–N(1)	2.044(4)
Zn(1)–O(2)	1.878(3)	Zn(3)–O(1)	2.059(3)
Zn(1)–O(3)	1.985(4)	Zn(3)–O(2a) ^a	1.907(3)
Zn(1)–O(12a)	1.912(4)	Zn(3)–O(6a)	2.174(4)
Zn(2)–O(1)	1.977(3)	Zn(3)–O(8)	1.939(4)
Zn(2)–O(4)	1.993(3)	Zn(3)–O(11a)	2.326(4)
Zn(2)–O(7a)	1.968(3)		
O(1)–Zn(1)–O(2)	106.3(1)	O(7a)–Zn(2)–N(1)	101.4(2)
O(1)–Zn(1)–O(3)	98.5(1)	O(1)–Zn(3)–O(2a)	106.1(1)
O(1)–Zn(1)–O(12a)	118.6(2)	O(1)–Zn(3)–O(6a)	91.3(1)
O(2)–Zn(1)–O(3)	111.4(2)	O(1)–Zn(3)–O(8)	105.0(1)
O(2)–Zn(1)–O(12a)	117.3(2)	O(1)–Zn(3)–O(11a)	90.6(1)
O(3)–Zn(1)–O(12a)	102.9(2)	O(2a)–Zn(3)–O(6a)	93.5(2)
O(1)–Zn(2)–N(1)	118.5(1)	O(2a)–Zn(3)–O(8)	148.8(2)
O(1)–Zn(2)–O(4)	105.9(1)	O(2a)–Zn(3)–O(11a)	92.2(1)
O(1)–Zn(2)–O(7a)	111.5(1)	O(6a)–Zn(3)–O(8)	87.6(1)
O(4)–Zn(2)–O(7a)	118.1(1)	O(6a)–Zn(3)–O(11a)	173.2(1)
O(4)–Zn(2)–N(1)	101.7(1)	O(8)–Zn(3)–O(11a)	85.7(1)

^a Symmetry code: (a) $-x + 1, y, -z + 1/2$.

**Figure 1.** Perspective view of the coordination environments of the zinc atoms.

independent zinc atoms (Figure 1). Zn(1) adopts a slightly distorted tetrahedral geometry, being coordinated by a μ_3 -OH group, a μ_2 -OH group, and two carboxylate oxygen atoms of two different 4,4'-oba ligands. Zn(2) also adopts a slightly distorted tetrahedral geometry, but it is coordinated by a μ_3 -OH group, two carboxylate oxygen atoms of two different 4,4'-oba ligands, and a nitrogen atom from 4,4'-bpy. Zn(3) resides in a distorted trigonal-bipyramidal environment, being coordinated by five oxygen atoms with a μ_3 -OH group, a μ_2 -OH group, and a carboxylate oxygen atom lying in an equatorial plane and two other carboxylate oxygen atoms in the axial positions. It should be noted that the μ_3 -OH group is not coplanar with the zinc atoms in the $Zn_3(\mu_3\text{-OH})$ core. The O1 atom is displaced 0.69 Å out of the Zn_3 plane.

The most remarked feature is that the $Zn_3(\mu_3\text{-OH})$ cores in **1** are interlinked together via the μ_2 -OH groups to generate an unprecedented helical $[Zn_3(\mu_3\text{-OH})(\mu_2\text{-OH})]_\infty$ chain, which

**Figure 2.** The helical chain of $[Zn_3(\mu_3\text{-OH})(\mu_2\text{-OH})]_\infty$ in **1**. Atom codes: C, shaded circle with highlight; O, open circle; N, circle with regular dot pattern; Zn, crosshatched circle. The broken lines represent hydrogen bonds (O9b–O1 2.806(5) Å, O9b–O2a 2.739(5) Å).**Figure 3.** Perspective view of the interconnection of the left- and right-handed helical chains.**Figure 4.** The three-dimensional framework of **1** viewed along the *b*-axis. Each 4,4'-bpy ligand is represented by a solid rod with a dotted circle at each end; each 4,4'-oba is represented by a V-shaped rod with an open circle at the middle and two carboxylate groups at the ends.

possesses a 2_1 screw axis (Figure 2). Presumably, the generation of helical chains in **1** may partially be attributed to the different coordination numbers of Zn(2) and Zn(3) and the bridging μ_2 -OH groups. Adjacent helical chains are interconnected by 4,4'-bpy ligands to generate a two-dimensional layer with left-handed helical (L) and right-handed helical (R) chains in a $\cdots L \cdots 4,4'$ -

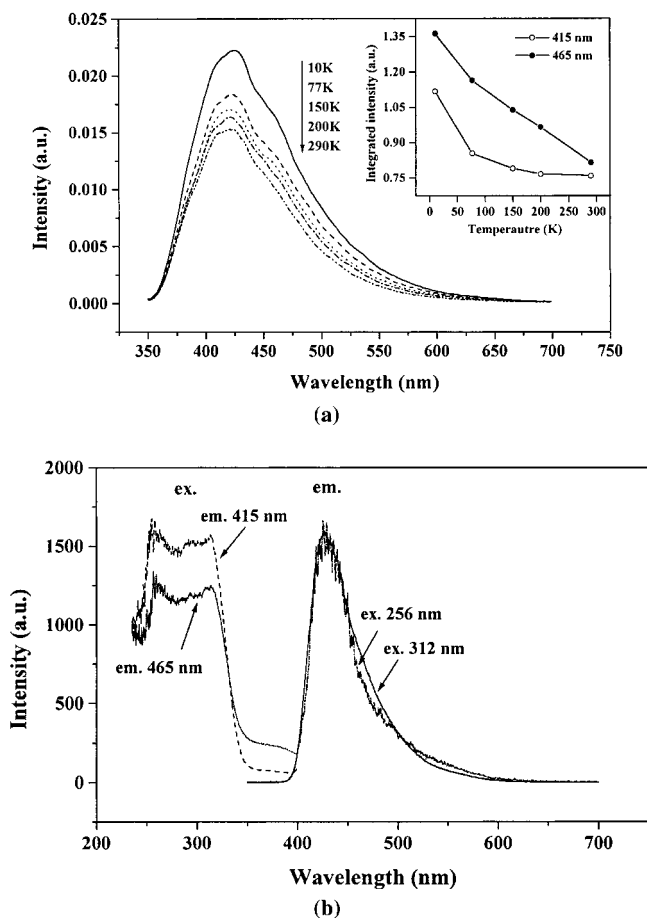


Figure 5. (a) Photoluminescence spectra and thermal-quenching curve (inset) of **1** at varied temperatures with excitation at 325 nm. (b) Emission and excitation spectra of **1** at room temperature.

bpy \cdots R \cdots 4,4'-bpy \cdots L \cdots mode (Figure 3). Here the 4,4'-bpy ligand may be important for stabilizing the helix because of its rigidity.¹¹ To our knowledge, no analogous two-dimensional coordination network consisting of polynuclear zinc helical chains and organic bridging ligands has been reported in the literature. There are two crystallographically independent 4,4'-oba ligands, one of which acts in a bis-bidentate fashion, and the other functions in a monodentate–bidentate fashion. The $[\text{Zn}_3(\mu_3\text{-OH})(\mu_2\text{-OH})(4,4'\text{-bpy})_{0.5}]_\infty$ layers are pillared by these dicarboxylate groups into a three-dimensional coordination architecture, as illustrated in Figure 4. The bridging carboxylate groups of 4,4'-oba play an important role in consolidating the trinuclear $\text{Zn}_3(\mu_3\text{-OH})$ cores and the helical chains, whereas the monodentate carboxylate group utilizes the uncoordinated oxygen atom to form two acceptor hydrogen bonds with the central $\mu_3\text{-OH}$ groups of an adjacent $\text{Zn}_3(\mu_3\text{-OH})$ core and a $\mu_2\text{-OH}$ group (see Figure 2), which may also enhance the stability of the helical chain.

Photoluminescent Properties. Complex **1** exhibits intense blue photoluminescence in the solid state. The emission spectra measured at varied temperatures consist of an asymmetrical and broad band with a shoulder on the longer wavelength side and a maximum at ca. 422 nm upon excitation at 325 nm (Figure

5a). From 290 to 10 K, a continuing increase in emission intensity is observed, while the emission energy and band shape remain constant. Each emission spectrum can be satisfactorily fitted with two Gaussian peaks centered at ca. 415 and 465 nm, respectively. They shift to longer wavelength only several nanometers with lowering the temperature from 290 to 10 K. The integrated intensities of the two peaks as a function of temperature are shown in the inset of Figure 5a. As the temperature drops from 290 to 10 K, the intensity of the band centered at ca. 465 nm increases linearly, whereas the increase of the band at ca. 415 nm is more significant at low temperature. Nevertheless, the temperature quenching effect for both bands is quite small.

The excitation and emission spectra at room temperature of **1** are shown in Figure 5b. The excitation spectra consist of two bands with the maxima at 256 and 312 nm, respectively. The emission spectrum excited with 256 nm radiation is similar to that excited with 312 nm radiation. The difference between the two emission bands implies that excitation in the 312 nm band is favorable to improving the intensity of the 465 nm emission.

In order to understand the nature of the two emission bands, we have confirmed that both free 4,4'-oba and 4,4'-bpy ligands do not emit any luminescence in the range 400–800 nm. Thus the emission of **1** might be attributable to the formation of the trinuclear clusters and/or ligand-to-metal charge transfer (LMCT).¹² Comparing the emission spectra of **1** with those of the Zn_4O unit in $[\text{Zn}_4\text{O}(\text{MeCO}_2)_6]$ and $\text{Zn}_4\text{B}_6\text{O}_{13}$,¹² we can ascribe the 415 nm band to the trinuclear clusters. The room-temperature excitation spectrum of **1**, with two strong bands, is very different from that of $\text{Zn}_4\text{B}_6\text{O}_{13}$, implying that the 4,4'-oba and/or 4,4'-bpy ligands participate in the process of energy transfer involved in the luminescence of **1**, and these organic ligands may contribute to the emission band at 465 nm.

Conclusions

A photoluminescent coordination polymer constructed with polynuclear zinc helical chains and mixed organic ligands has been prepared and characterized. The helical chains are interlinked with 4,4'-bpy to generate 2D networks, which are then pillared by 4,4'-oba spacers. The compound can be excited directly and through an energy transfer process from the organic ligands to emit strong luminescence at room temperature, on which the temperature quenching effect is very small.

Acknowledgment. This work was supported by the NSFC (29971033 & 20001008) and Foundation for University Key Teacher of the Ministry of Education of China.

Note Added after ASAP. An error appeared in the version of this paper that was posted on Sep 25, 2001. In the second paragraph of the section Photoluminescent Properties, the third sentence has been corrected to read, "The emission spectrum excited with 256 nm radiation is similar to that excited with 312 nm radiation."

Supporting Information Available: X-ray crystallographic file in CIF format. This material is available free of charge via the Internet at <http://pubs.acs.org>.

IC010472U

(11) Shi, Z.; Feng, S.-H.; Gao, S.; Zhang, L.-R.; Yang, G.-Y.; Hua, J. *Angew. Chem., Int. Ed.* **2000**, *39*, 2325.

(12) (a) Meijerink, A.; Blasse, G.; Glasbeek, M. *J. Phys.: Condens. Matter* **1990**, *2*, 6303. (b) Bertonecello, R.; Bettinelli, M.; Cassrin, M.; Gulino, A.; Tondello, E.; Vittadini, A. *Inorg. Chem.* **1992**, *31*, 1558.